Molecular Therapy
Oncology
Original Article

Stratifying hepatocellular carcinoma based on immunophenotypes for immunotherapy response and prognosis

Yunpeng Liu,[1,3] Hongchen Ji,[1,3] Li-Hong Wu,[2,3] Xiang-Xu Wang,[1,3] Yue Yang,[1] Qiong Zhang,[1] and Hong-Mei Zhang[1]

[1]Department of Clinical Oncology, Xijing Hospital, Fourth Military Medical University, Xi'an, Shaanxi 710032, China; [2]Department of Gastroenterology, Xijing 986 Hospital, Fourth Military Medical University, Xi'an, Shaanxi 710032, China

Immunotherapy has transformed the management of hepatocellular carcinoma (HCC), but effectiveness varies among patients. This study aimed to identify biomarkers and HCC subtypes responsive to immunotherapy. Patients were classified into Immunity-High (Immunity-H) and Immunity-Low (Immunity-L) subtypes using ssGSEA scores. Prognostic genes were identified through Cox regression, and immune cell infiltration was quantified with TIMER 2.0. Brother of CDO (BOC) expression, analyzed via immunohistochemistry, correlated with immunotherapy responses. Flow cytometry assessed immune cell infiltration relative to BOC levels, while CCK-8 and transwell assays evaluated BOC overexpression's effects on cell proliferation and invasiveness. Clinically, immunity-H patients had better survival outcomes. Three hub genes—BOC, V-Set and Transmembrane Domain Containing 1 (VSTM1), and PRDM12—were identified as significantly associated with prognosis. Among these, BOC and VSTM1 demonstrated positive correlations with immune cell infiltration. Elevated expression of BOC was found to be predictive of favorable responses to immunotherapy and was associated with enhanced infiltration of T cells, dendritic cells, and B cells in the tumor microenvironment. Conversely, BOC overexpression in liver cancer cell lines led to decreased cell proliferation and invasiveness. This study underscores the prognostic significance of HCC subtypes defined by immunogenomic profiles and identifies BOC as a potential biomarker for immunotherapy selection and outcome prediction.

INTRODUCTION

Hepatocellular carcinoma (HCC) is the third highest contributor to cancer-related mortality worldwide.[1] HCC is characterized by an insidious onset, high recurrence rates, and poor prognosis, and it presents a formidable challenge in oncology. In addition to liver transplantation and localized treatments such as ablation and transarterial chemoembolization, systemic therapy remains a key option for patients with locally advanced or metastatic HCC. While sorafenib and lenvatinib have traditionally been the first-line systemic therapies, the development of immune checkpoint inhibitors (ICIs) has significantly transformed the treatment landscape.[2–4] Although immunotherapy has transformed the management of cancer, its therapeutic impact on HCC is limited. The overall survival (OS) rate at 48 months post-treatment is only 25.2%.[5] The main issues with the application of immunotherapy in HCC patients are a poor treatment response, accelerated tumor progression, and immune-related adverse events.[6] Although many biomarkers, including programmed death-ligand 1 (PD-L1) expression, tumor mutation burden, and different genomic changes, have been identified, their predictive utility has been compromised due to the inherent heterogeneity of tumors.[7–11] These findings emphasize the urgent need to identify more reliable biomarkers that can enhance the effectiveness of ICI therapy and alleviate adverse reactions in HCC patients.

The tumor microenvironment (TME) has attracted considerable attention in recent oncological research. The progression of HCC is significantly influenced by the TME, which is composed of a complex network of immune and nonimmune stromal cells.[12] Previous studies have shown that the composition and behavior of tumor-infiltrating immune cells are key factors affecting patient prognosis and the effectiveness of immunotherapy interventions.[13,14] For example, a better prognosis is usually associated with the presence of $CD8^+$ T cells in the TME, whereas a poorer prognosis is usually associated with the presence of M2 polarized macrophages and other immunosuppressive cells.[15] Consequently, in-depth research on the TME is expected to not only reveal the pathogenesis of HCC but also pave the way for the discovery of new immunotherapy targets.

In this study, we classified HCC into Immunity-High (Immunity-H) subtypes and Immunity-Low (Immunity-L) subtypes and then analyzed 29 immune genome maps via single-sample gene set enrichment analysis (ssGSEA). Next, we investigated the different molecular characteristics and differences between these subtypes, investigating the

Received 13 June 2024; accepted 2 October 2024;
https://doi.org/10.1016/j.omton.2024.200890.

[3]These authors contributed equally

Correspondence: Hong-Mei Zhang, Department of Clinical Oncology, Xijing Hospital, Fourth Military Medical University, Xi'an, Shaanxi 710032, China.
E-mail: zhm@fmmu.edu.cn

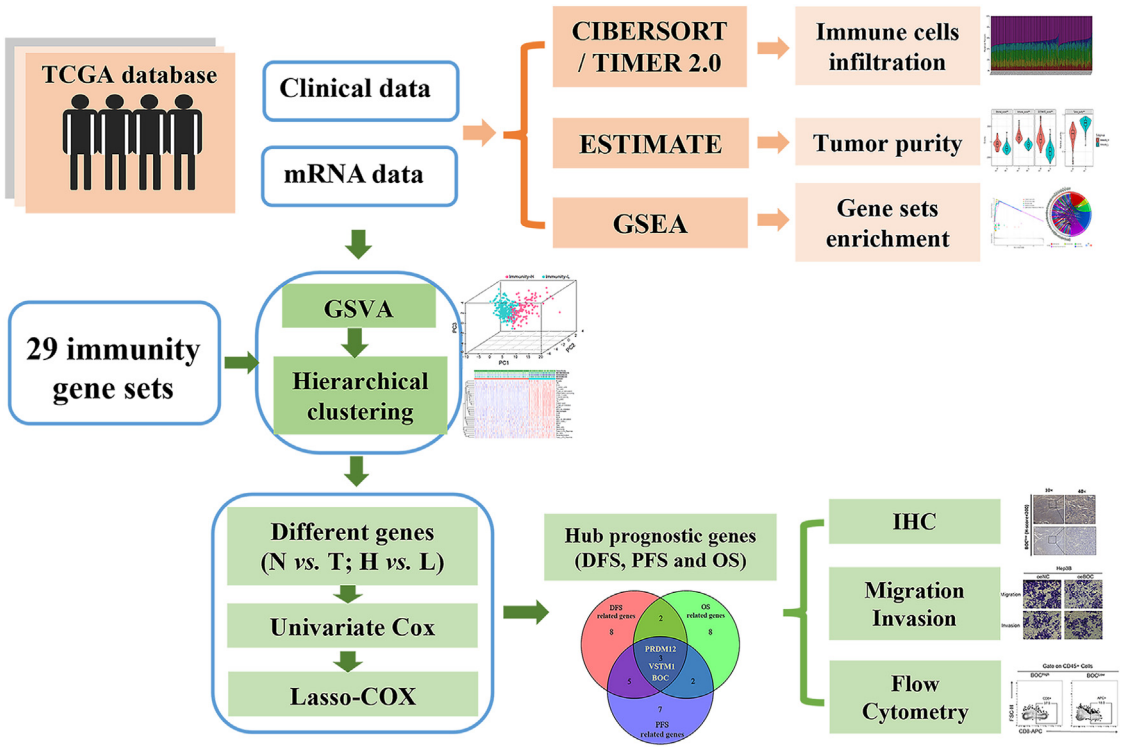

Figure 1. Analysis flowchart

Clinical and gene expression data of 371 HCC samples from TCGA. Immune cell infiltration proportions and tumor purity for each sample were estimated using the CIBERSORT and ESTIMATE algorithms. Immune cell infiltration data were further analyzed with TIMER 2.0. GSVA scores were calculated based on the expression levels of 29 immune-related gene sets, and samples were classified into Immunity-H and Immunity-L subtypes using hierarchical clustering. DEGs between normal and tumor samples, as well as between Immunity-H and Immunity-L subtypes, then univariate Cox and LASSO-based Cox were used to identify DFS, PFS, and OS prognostic genes. Core prognostic genes were determined by the intersection of DFS, PFS, and OS prognostic gene sets.

distribution of immune cell infiltration, gene set enrichment, and the efficacy of immunotherapy. Our research revealed that the expression of Brother of Cell Adhesion Molecule-Related/Downregulated by Oncogenes (CDO) (BOC) is positively correlated with the levels of $CD4^+$ T cells, $CD8^+$ T cells, dendritic cells (DCs), and B cells in HCC tumor tissue. In addition, we observed a significant correlation between the expression of BOC and improved immunotherapeutic efficacy. Through further analysis and *in vitro* experiments, the expression of BOC in HCC tumor tissue was confirmed to be directly positively correlated with the presence of a series of immune cells, including $CD4^+$ T cells, $CD8^+$ T cells, DCs, and B cells. Furthermore, a significant association was observed between BOC expression and positive outcomes in patients receiving immunotherapy. Our findings will facilitate the stratification of HCC patients on the basis of immunogenomic signatures and biomarkers, potentially offering a robust framework for tailoring immunotherapeutic strategies.

RESULTS

Immunity subtype identification and clinical features of HCC patients

Our analytical pipeline, as illustrated in Figure 1, commenced with the extraction of gene expression data (quantified as fragments per kilobase million [FPKM]) from 371 HCC samples within The Cancer Genome Atlas (TCGA) cohort. Subsequently, we performed ssGSEA on 29 immunogenomic profiles. Unsupervised clustering analysis, based on the resultant ssGSEA scores (Figures S1A–S1D), revealed two distinct sample clusters, as evidenced by the hierarchical clustering dendrogram and principal-component analysis plot (Figure S1E). These clusters were characterized by high and low immune signatures, leading to the identification of two discrete immune subtypes, which we designated Immunity-H and Immunity-L, respectively.

The heatmap comparison revealed significantly higher ssGSEA scores for immune-related gene sets in Immunity-H compared to Immunity-L (Figure 2A; $p < 0.001$, Student's t test). Further analysis of additional immune signatures, including stromal score, immune score, and the total Estimation of Stromal and Immune cells in Malignant Tumor Tissues Using Expression Data (ESTIMATE) score, confirmed that all three metrics were markedly elevated in Immunity-H (Figure 2B; all $p < 0.001$). Conversely, tumor purity was found to be lower in Immunity-H than in Immunity-L (Figure 2C; $p < 0.001$), suggesting distinct TMEs between the subtypes, with Immunity-H exhibiting stronger antitumor immune signatures.

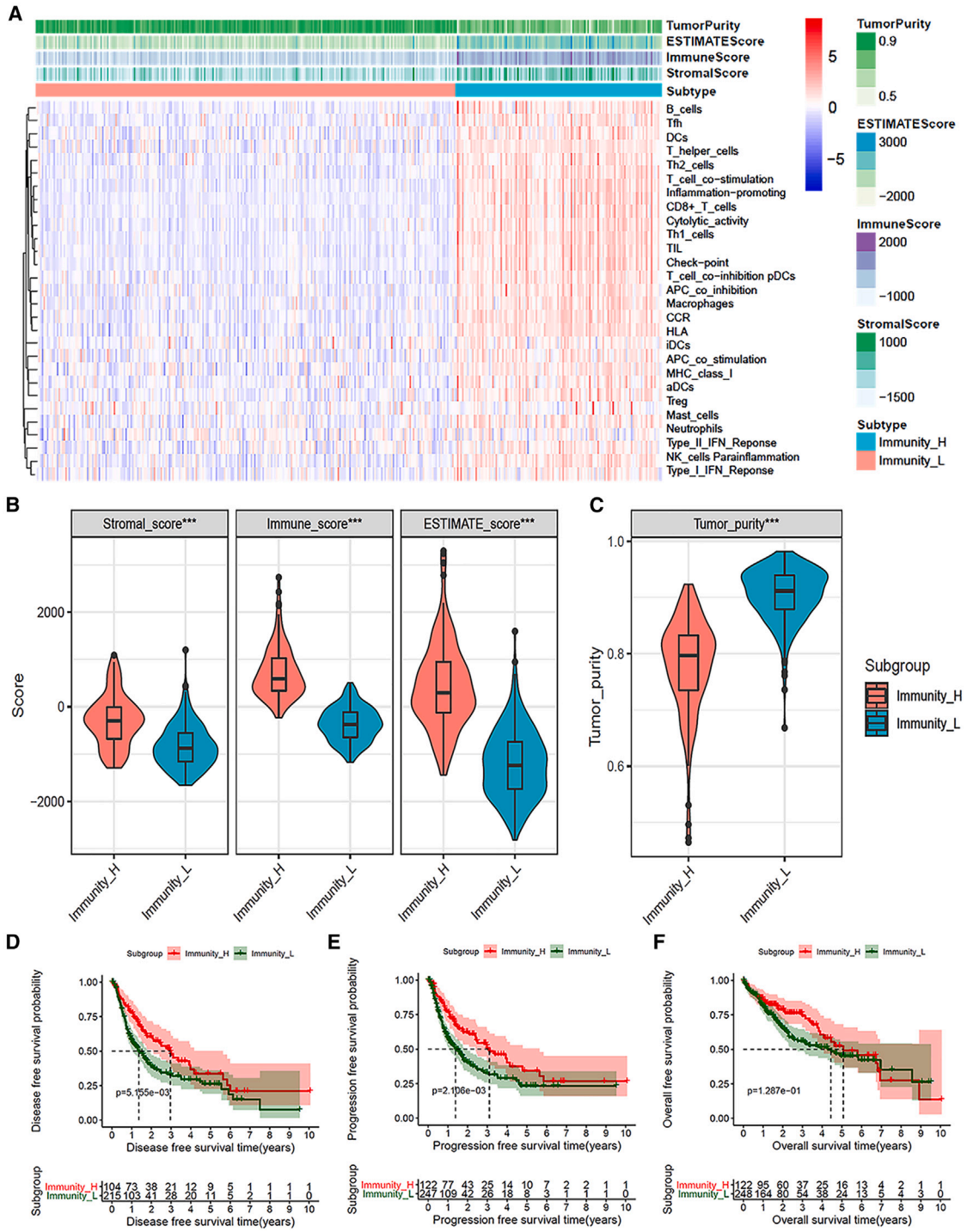

Figure 2. Hierarchical clustering of HCC samples base on 29 immunity-related gene sets

(A) The hierarchical clustering heatmap illustrates the GSVA enrichment scores for immunity-related gene sets in 371 HCC samples, categorized into Immunity-H and Immunity-L subgroups. Atop the heatmap, color bars represent the tumor purity, ESTIMATE score, immune score, and stromal score, determined by the ESTIMATE algorithm. (B and C) Comparative analysis of the immunity subtypes is presented through violin plots, showcasing differences in estimated scores, stromal scores, immune scores, and tumor purity. (D–F) The Kaplan-Meier method provides survival analysis for DFS, PFS, and OS between the immunity subtypes, utilizing the log rank test for statistical significance.

Table S1 presents the clinical characteristics of 123 Immunity-H and 248 Immunity-L patients. No significant differences were observed in age, gender, race, vascular invasion, or serum α-fetoprotein levels ($p > 0.05$, chi-squared test), except for American Joint Committee on Cancer (AJCC) stage. The AJCC stage analysis showed a higher proportion of stage I/II in Immunity-H (97 [78.9%]) compared to Immunity-L (160 [64.5%]), with fewer patients at stage III/IV (Immunity-H: 20 [16.3%] vs. Immunity-L: 70 [28.2%]) and unspecified stages (Immunity-H: 6 [4.9%] vs. Immunity-L: 18 [7.3%]) ($p = 0.018$, chi-squared test).

Kaplan-Meier survival analysis indicated a significant clinical advantage for Immunity-H patients, as evidenced by longer disease-free survival (DFS), progression-free survival (PFS), and OS (Figures 2D–2F; DFS: $p = 0.005$, PFS: $p = 0.002$, OS: $p = 0.129$; log rank test). These findings align with previous reports suggesting that enhanced antitumor immune signatures show a correlation with improved survival outcomes.[16]

HCC immunity subtypes are tightly related to HLA and immune checkpoint-related genes

Further analysis focused on the differential expression of human leukocyte antigen (HLA) and immune checkpoint genes across the identified subgroups. Notably, the Immunity-H subtype demonstrated significantly elevated expression levels of multiple immune checkpoint genes, including CTLA4, PD-L1 (CD274), PD-L2 (PDCDLG2), IDO1, and IDO2, compared to the Immunity-L subtype (Figure S2A; all $p < 0.001$). A similar pattern was observed in the expression profiles of HLA-related genes, encompassing HLA-A, HLA-B, HLA-C, and HLA-DMA (Figure S2B; all $p < 0.001$). These findings were consistent across all examined genes and statistically significant. Collectively, these results highlight a robust association between the identified immune subtypes and the expression patterns of key immune-related genes in HCC, providing further molecular characterization of the immunological differences between these subtypes.

Immune cell infiltration and GSEA were compared between the two distinct immunity subtypes

Using the CIBERSORT algorithm, we evaluated the differences in the TME between subtypes of HCC. Analysis of immune cell infiltration (Figures 3A and S3A) demonstrated that the Immunity-H subtype was characterized by significantly increased infiltration of plasma B cells, activated $CD4^+$ T cells, $CD8^+$ T cells, γδ T cells, follicular helper T cells, M1 macrophages, activated natural killer (NK) cells, and resting myeloid DCs ($p < 0.05$, Wilcoxon test). In contrast, the Immunity-L subtype exhibited a higher concentration of naive B cells, M2 macrophages, activated myeloid DCs, and $CD4^+$ T cells ($p < 0.05$, Wilcoxon test).

Corroborating these findings, the TIMER 2.0 database analysis of six immune cell types (Figures S3B and S3C) indicated a similar pattern. In Immunity-H, the infiltration levels of B cells, $CD8^+$ T cells, and macrophages were significantly increased (all $p < 0.05$, Wilcoxon test), whereas $CD4^+$ T cells, neutrophils, and myeloid DCs showed a significant decrease (all $p < 0.05$, Wilcoxon test).

Furthermore, Kyoto Encyclopedia of Genes and Genomes (KEGG) and Hallmark GSEA revealed that Immunity-H was associated with an enriched immune activation pathway. This included pathways such as interferon-γ response, NK-mediated cytotoxicity, chemokine signaling, primary immunodeficiency, and inflammatory response (Figures 3B and 3C).

Analysis of gene mutations and expression differences between two immunity subtypes

To investigate the potential mechanisms underlying the distinction between the two HCC immune subtypes, we analyzed the mutation distribution of the top 20 genes exhibiting the highest mutation frequency in HCC. This analysis was conducted by stratifying the data between the immunity-H and immunity-L subtypes (Figure S4A). Intriguingly, the immunity-H subtype exhibited a lower frequency of titin (TNN) mutations. Although not reaching statistical significance, patients harboring TNN mutations demonstrated a trend toward poorer OS, PFS, and DFS (Figures S4B–S4D; $p = 0.355$, $p = 0.121$, and $p = 0.293$, respectively, using the log rank test).

Furthermore, we assessed the neoantigen landscape by comparing SNVs, indel mutations, non-silent mutation frequencies, and silent mutation frequencies across the two immune subtypes. Contrary to expectations, these comparisons revealed no statistically significant differences in gene mutation profiles between the immune subtypes of liver cancer (Figures S4E–S4H; all $p > 0.05$, Wilcoxon test).

Advancing our investigation, we scrutinized the differential gene expression between HCC and adjacent normal tissue. The heatmap and volcano plot analyses disclosed that relative to adjacent non-tumorous tissue, 4,942 genes were significantly upregulated (log2 fold change [FC] >1, false discovery rate [FDR] <0.05), while 540 genes were substantially downregulated (log2 FC <−1, FDR <0.05) in HCC (Figures S5A and S5B). Leveraging these 5,482 differentially expressed genes (DEGs), we delved into the expression disparities between the two immunity subtypes. The results elucidated that compared to immunity-L, immunity-H is characterized by 174 significantly upregulated genes (log2 FC >1, FDR <0.05) and 30 markedly downregulated genes (log2 FC <−1, FDR <0.05) (Figures S5C and S5D).

To elucidate the biological processes differentially represented between the HCC Immunity-H and Immunity-L subtypes, we performed GSEA using Gene Ontology (GO) terms. This analysis revealed a significant upregulation of immune-related pathways in the Immunity-H subtype. Specifically, we observed enrichment in pathways associated with the major histocompatibility complex (MHC) class II protein complex, NK cell chemotaxis, complement receptor activity, and negative regulation of myeloid leukocyte-mediated immunity (Figures 4A and 4B). These findings were statistically significant (FDR <0.05) and provide strong support for enhanced immune activation in the Immunity-H subtype. The differential

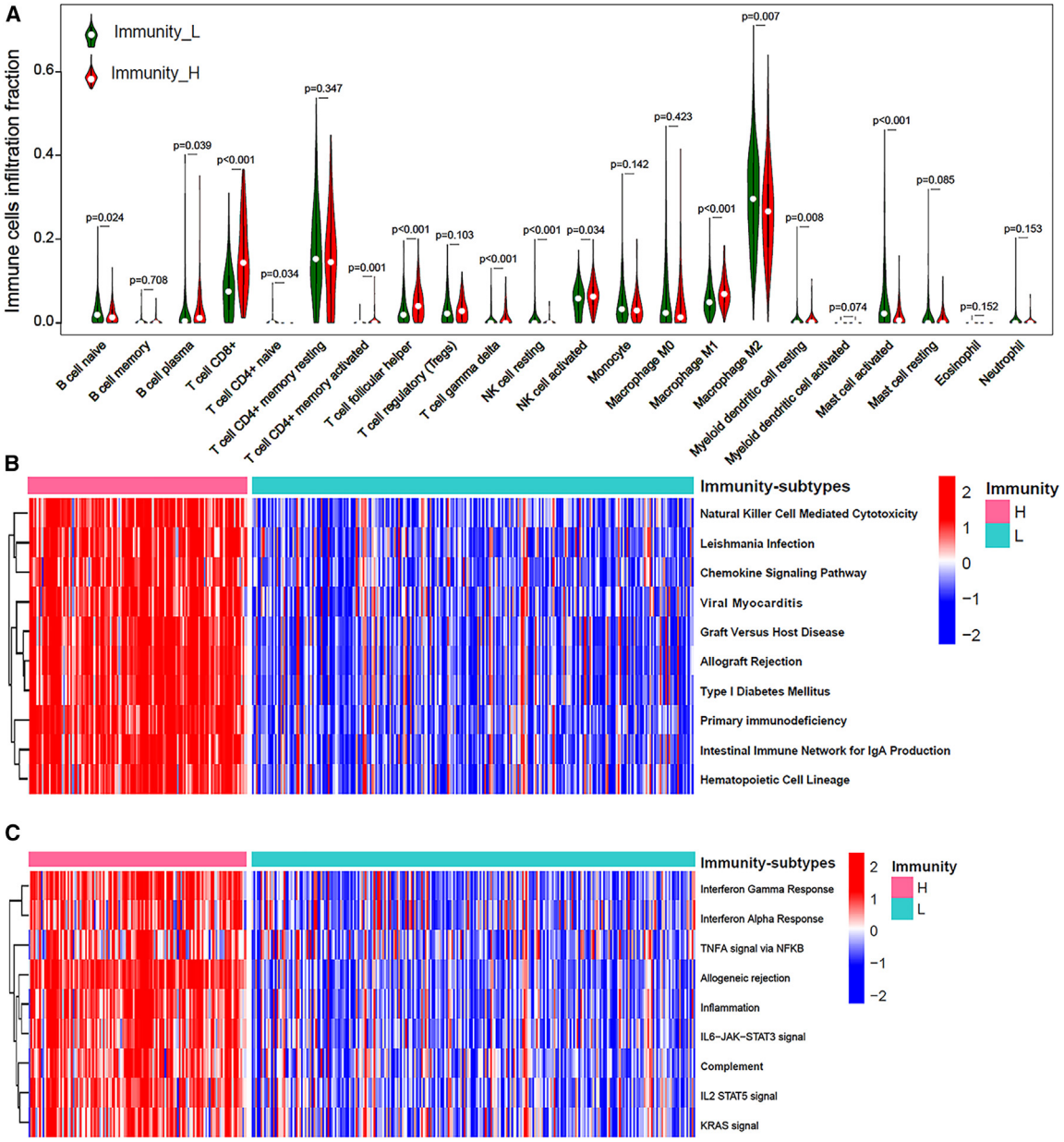

Figure 3. Differential analysis of immune cell infiltration and GSEA scores across immunity subtypes

(A) An assessment of 22 immune cell types was conducted to discern differences in infiltration between the immunity subtypes, utilizing the CIBERSORT algorithm and the Wilcoxon test for analysis. (B and C) The heatmap depicts the GSVA scores for selected KEGG and Hallmark pathways, as compiled from MSigDB, across two immune subtypes.

enrichment of these immune-related processes underscores the distinct immunological landscapes characterizing these two HCC subtypes and offers potential mechanistic insights into their divergent clinical behaviors.

HCC prognosis significant gene screening

To elucidate the mechanisms underlying HCC onset and progression, we performed univariate Cox regression analysis on DFS, PFS, and OS using 204 DEGs identified in our previous analysis. Genes with significant prognostic value were further refined using least absolute shrinkage and selection operator (LASSO)-based Cox regression, yielding 15 genes associated with OS (Figures S6A–S6C), 17 with PFS (Figures S6D–S6F), and 18 with DFS (Figures S6G–S6I). Notably, three genes—BOC, V-Set and Transmembrane Domain Containing 1 (VSTM1), and PR/SET Domain 12 (PRDM12)—were consistently implicated across all survival outcomes (Figure 4C).

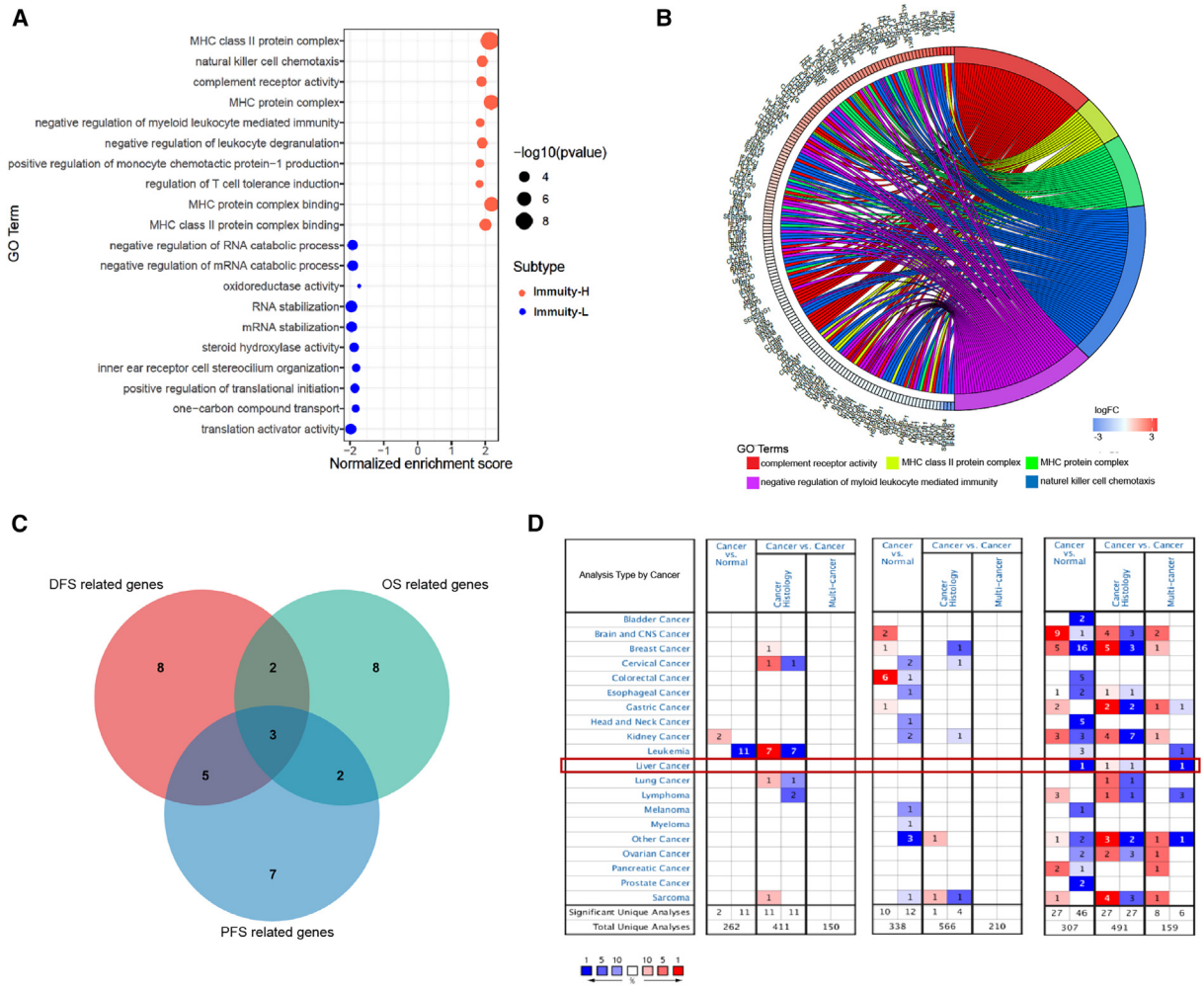

Figure 4. GSEA of HCC immunity subtype-specific GO term and prognosis significant genes screening

(A and B) Enrichment plot (A) and (B) enrichment circle graph of top 5 GO terms enriched in the Immunity-H subtype. (C) Venn diagram illustrating the intersection of genes associated with DFS, PFS, and OS. Three prognostic hub genes—BOC, PRDM12, and VSTM1—are shared among DFS, PFS, and OS. (D) The illustration presents the count of datasets exhibiting statistically significant upregulation (indicated in red) or downregulation (shown in blue) in mRNA levels of VSTM1, PRDM12, and BOC within the Oncomine database ($p < 0.05$, |log FCl >2).

Expression patterns of these overlapping genes across various cancer types were investigated using the Oncomine database. VSTM1 was found to be frequently underexpressed in leukemia, while PRDM12 was often overexpressed in colorectal cancer. Interestingly, both VSTM1 and PRDM12 have been infrequently reported in the oncology literature and have not been previously associated with liver cancer. In contrast, BOC is more commonly studied in tumor research, showing high expression in brain, CNS, and kidney cancers, but low expression in breast, bladder, prostate, and head and neck tumors. Only one study has reported low BOC expression in liver cancer (Figure 4D).

Analysis of the three pivotal genes using the TCGA database revealed distinct expression profiles between cancerous and normal tissues, as well as across the two independent HCC immunity subtypes (Figures S7A and S7B). BOC and PRDM12 were significantly upregulated in tumor tissues, whereas VSTM1 was downregulated ($p < 0.001$, Student's t test). Moreover, BOC and VSTM1 exhibited marked overexpression in the immunity-H subtype, while PRDM12 expression was significantly reduced ($p < 0.001$, Student's t test).

Kaplan-Meier survival analysis and verification of BOC, VSTM1, and PRDM12

We investigated the prognostic value of BOC, VSTM1, and PRDM12 gene expressions. Kaplan-Meier survival analyses for OS, PFS, and DFS indicated that high expression levels of BOC were associated with a favorable prognosis trend (Figures 5A–5C; BOC: $p < 0.05$, log rank test). Conversely, high expression levels of PRDM12 and

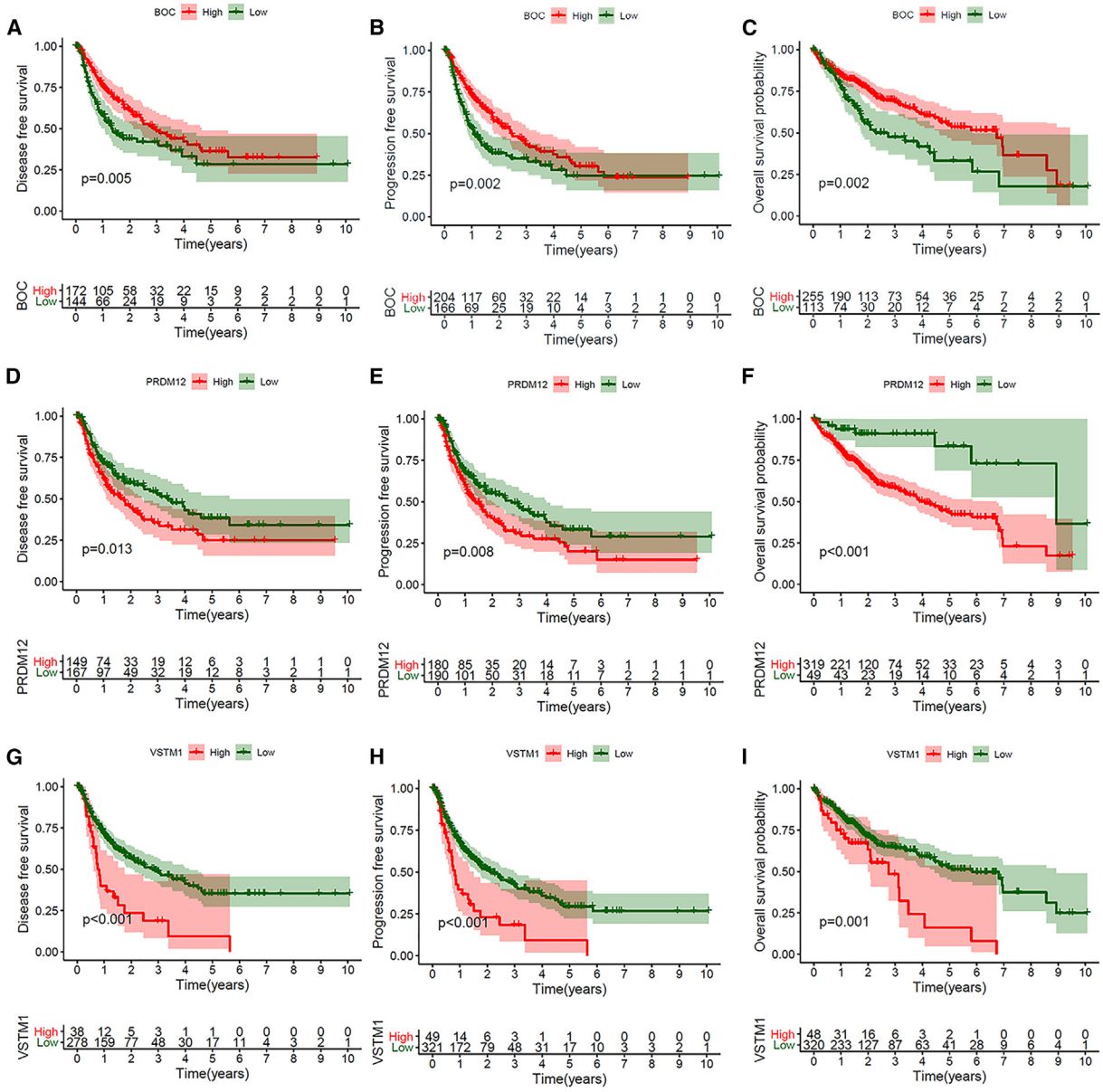

Figure 5. Prognostic feature of three hub genes expression in HCC patients

(A–C) The DFS (A), (B) PFS, and (C) OS curves illustrate a comparison between HCC patients exhibiting high BOC gene expression (indicated in red) and those with low expression (shown in dark green). (D–F) DFS (D), (E) PFS, and (F) OS curves display the comparison of HCC patients with high (red) vs. low (dark green) PRDM12 gene expression. (G–I) DFS (G), (H) PFS, and (I) OS curves delineate the outcomes for HCC patients categorized by high (indicated in red) and low (shown in dark green) expression levels of the BOC gene, as analyzed by the log rank test. The cutoff points for categorizing gene expression into high and low subgroups were determined using the R package "survival" and "surv_cutpoint" function.

VSTM1 were associated with an unfavorable prognosis trend (Figures 5D–5I; PRDM12 and VSTM1: $p < 0.05$, log rank test).

Further validation using the International Cancer Genome Consortium (ICGC) database confirmed similar trends for PRDM12 and BOC (Figures S8A and S8B; $p = 0.007$ and $p = 0.065$, log rank test), while VSTM1 expression did not show a significant correlation with HCC prognosis (Figure S8C; $p = 0.692$, log rank test), possibly due to tumor heterogeneity and sample variability.

Our findings were corroborated by analysis of the GSE76427 dataset, which demonstrated that patients with high BOC expression tended toward better DFS and OS (Figures S8D and S8G; $p = 0.155$ and $p = 0.067$, log rank test). Patients with high PRDM12 expression

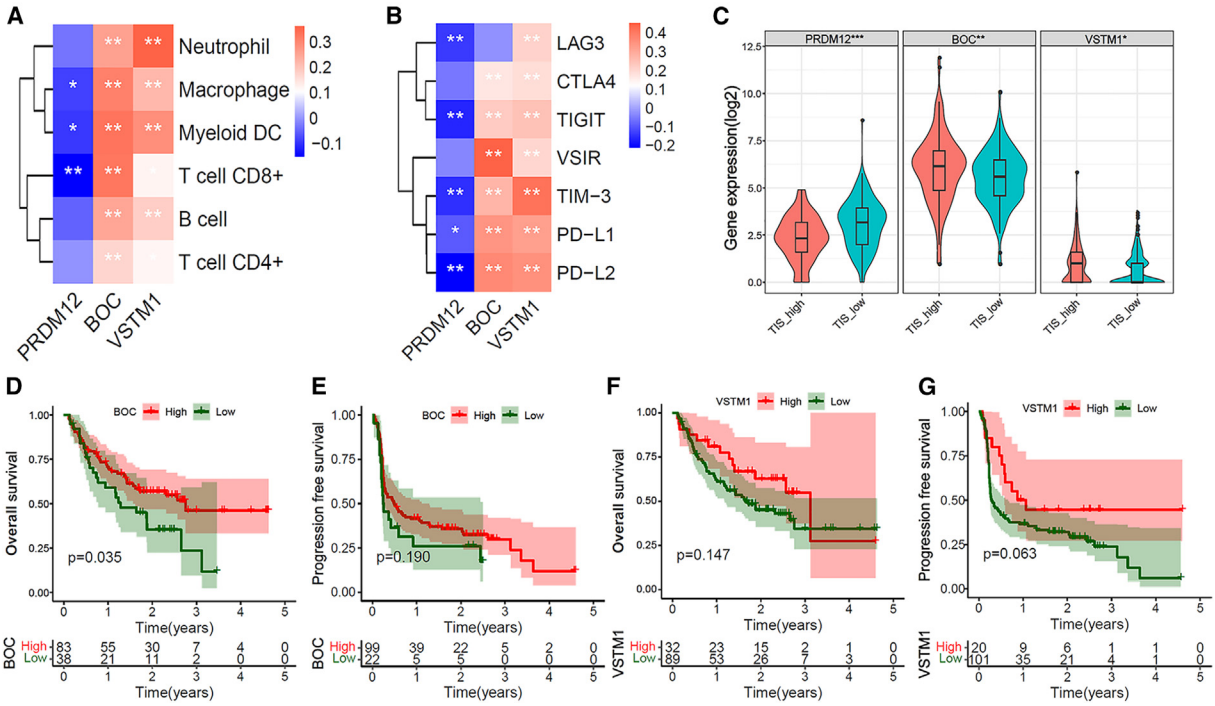

Figure 6. Three hub genes expression was associated with the efficacy of immune checkpoint therapy

(A) Heatmap illustrating the correlation between the expression levels of BOC, VSTM1, and PRDM12 genes and the infiltration levels of six immune cell types. (B) Heatmap showing the correlation between BOC, VSTM1, and PRDM12 gene expression and immune checkpoint gene expression (Spearman correlation test; $^{*}p < 0.05$; $^{**}p < 0.01$; $^{***}p < 0.001$). (C) Comparison of six immune cells infiltration in two immunity subtypes (Wilcoxon test; $^{*}p < 0.05$; $^{**}p < 0.01$; $^{***}p < 0.001$). (D and F) OS curves comparing patients with (D) BOC gene and (F) VSTM1 gene high (red) and low (dark green) expression in the Liu et al. cohort. (E and G) PFS curves comparing patients with (E) BOC gene and (G) VSTM1 gene high (red) and low (dark green) expression in the Liu et al. cohort.

showed a tendency toward poorer DFS and OS (Figures S8E and S8H; $p = 0.079$ and $p = 0.059$, log rank test). In contrast, high VSTM1 expression was associated with worse DFS prognosis and no significant difference in OS (Figures S8F and S8I; $p = 0.048$ and $p = 0.886$, log rank test).

Patients with BOC and VSTM1 high expression indicate better immunotherapy efficacy

To elucidate the relationship between BOC, VSTM1, and PRDM12 genes and immunotherapy efficacy, we first examined their expression correlation with immune cell infiltration and immune checkpoint molecule expression. TIMER analysis revealed significant positive correlations between BOC and VSTM1 expression levels and the presence of $CD4^+$ T cells, $CD8^+$ T cells, B cells, neutrophils, and macrophages ($p < 0.05$, Spearman's correlation test). Conversely, PRDM12 expression exhibited a significant inverse relationship with $CD8^+$ T cells and macrophages, as detailed in Figure 6A ($p < 0.05$, Spearman's correlation test). Consistent with these findings, BOC and VSTM1 expression levels demonstrated significant positive correlations with key immune checkpoint molecules, including CTLA4, PD-L1, PD-L2, TIM-3, TIGIT (T cell immunoreceptor with immunoglobulin [Ig] and ITIM domains), and VSIR. In contrast, PRDM12 expression showed significant negative correlations with these immune checkpoints (Figure 6B; $p < 0.05$, Spearman's correlation test). These results collectively suggest divergent roles for BOC and VSTM1 versus PRDM12 in modulating the tumor immune microenvironment and checkpoint inhibitor expression in HCC.

Subsequent analysis focused on the expression levels of PRDM12, BOC, and VSTM1 in subgroups with high and low Tumor Inflammation Signature (TIS), which is known to be associated with the response to immunotherapy. The findings indicated that BOC and VSTM1 expressions were significantly elevated in the TIS-high subgroup, while PRDM12 was markedly reduced (Figure 6C; $p < 0.05$, Student's t test), suggesting that high BOC and VSTM1 expressions are indicative of a potential immunotherapy benefit, whereas PRDM12 may signal poor immunotherapy efficacy.

In an independent immunotherapy cohort (Liu et al. cohort), we confirmed the therapeutic advantage of BOC and VSTM1, as PRDM12 data were not available. Patients with high expressions of BOC and VSTM1 experienced improved OS outcomes (Figures 6D and 6F; $p = 0.035$ and $p = 0.147$, log rank test) and favorable PFS outcomes (Figures 6E and 6G; $p = 0.190$ and $p = 0.063$, log rank test).

Elevated BOC expression correlates with favorable anti-PD-1 therapy outcomes and enhanced CD8$^+$ T cell infiltration in HCC

To evaluate the clinical relevance of BOC expression in immunotherapy response, we conducted a retrospective study on 10 patients with HCC who received anti-PD1 monotherapy after surgical resection (Barcelona Clinic Liver Cancer stage A). The patient characteristics are summarized in Table S2. Immunohistochemical (IHC) staining was performed to assess BOC protein expression levels in tissue sections from these patients (Figure 7A). Notably, patients with high BOC expression (H-score >200) exhibited a lower 1-year recurrence rate (20%, 1/5) compared to those with low BOC expression (H-score <200; 60%, 3/5), suggesting a positive correlation between BOC expression and ICI efficacy in HCC patients.

To further investigate the relationship between BOC expression and the tumor immune microenvironment, we analyzed fresh tissue specimens from six HCC patients. BOC protein expression was assessed by western blot (Figure 7B), and immune cell infiltration was quantified using flow cytometry. In tumors with high BOC protein expression (cases 1, 5, and 6), we observed significantly higher infiltration rates of CD8$^+$ T cells, DCs, CD4$^+$ T cells, and B cells compared to tumors with low BOC expression (cases 2–4) (Figures 7C and 7D). These findings indicate a positive association between BOC expression levels and immune cell infiltration in the HCC TME.

Collectively, our data consistently demonstrate a positive correlation between BOC expression and the infiltration of CD4$^+$ T cells, CD8$^+$ T cells, DCs, and B cells within the HCC TME. These results suggest that BOC expression may serve as a potential biomarker for predicting favorable responses to ICI therapy in HCC patients.

BOC overexpression attenuates proliferative and migratory capacities in HCC cell lines

To delineate the functional role of BOC in HCC, we overexpress the BOC gene in the Hep3B and MHCC97H cell lines. We confirmed the successful upregulation of BOC expression via western blot, as depicted in Figure 8A. Cell viability was assessed utilizing a CCK-8 assay. The data indicated that BOC overexpression markedly suppressed the proliferation of both Hep3B and MHCC97H cells, as illustrated in Figure 8B. Furthermore, enhanced BOC expression was found to considerably diminish the migratory and invasive properties of these HCC cell lines, as evidenced by transwell migration and invasion assays, which is evidenced in Figures 8C and 8D.

DISCUSSION

The TME has been recognized increasingly as playing a crucial role in influencing tumor progression and treatment responses.[17,18] Genomic mapping has been instrumental in the identification of molecular subtypes across a spectrum of cancers.[19,20] HCC is characterized by its marked heterogeneity and aggressive malignancy. In light of the HIMALAYA study, the National Comprehensive Cancer Network guidelines advocate for the combination of tremelimumab and durvalumab for the treatment of HCC, but the objective response rate remains modest at 20.1%.[21] These findings highlight the importance of developing an immune-related classification for HCC to increase the efficacy of immunotherapeutic interventions.

In our investigation, we delineated two discrete immune subtypes of HCC, each associated with a distinct immune microenvironment. The Immunity-H subtype was distinguished by a profusion of infiltrating immune cells, notably CD8$^+$ T cells, and stromal elements, coupled with low tumor purity and a significant prognostic outlook. In addition, the overexpression of HLA and immune checkpoint genes was observed in the Immunity-H subtype. Therefore, we postulate that patients with Immunity-H subtype HCC are more likely to respond to immunotherapy strategies. To investigate the potential mechanisms of the different HCC immune subtypes, comparative gene expression analysis was conducted. This analysis involved HCC and normal tissues, as well as the two immune subtypes. A total of 204 genes were significantly differentially expressed in the two immune subtypes, and GO enrichment analysis revealed that immune-related pathways were significantly enriched in the Immunity-H subtype. These findings confirm the activation of the immune microenvironment in the Immunity-H subtype.

Accumulating evidence suggests that enhanced immune activation is prognostically favorable across various tumor types.[22,23] In our investigation, patients assigned to the Immunity-H subgroup exhibited better DFS, PFS, and OS. To identify genes with significant prognostic value, we conducted univariate Cox and LASSO-based Cox analyses on DFS, PFS, and OS with 204 DEGs. This analysis identified BOC, VSTM1, and PRDM12 as key prognostic genes. Kaplan-Meier survival curves revealed that high expression of BOC was correlated with improved DFS, PFS, and OS, whereas elevated levels of VSTM1 and PRDM12 were indicative of poorer outcomes.

This study revealed a significant positive relationship between the expression of BOC and the abundance of immune cells and the expression of immune checkpoint-related molecules. Conversely, PRDM12 expression exhibited an inverse relationship. These findings suggest that high BOC expression may serve as a biomarker of a favorable prognosis and as a predictor of an enhanced response to immunotherapy. Conversely, high PRDM12 expression may be associated with a poor prognosis and diminished immunotherapy efficacy. Interestingly, while high VSTM1 expression constitutes a prognostic risk factor, it may also indicate a better response to immunotherapy. Previous reports have linked VSTM1 to T helper 17 cell activation.[24] Given the emerging role of VSTM3 (TIGIT) as an immune checkpoint that modulates T cell functions and tumor immunotherapy, our results suggest that VSTM1 could be a novel immune checkpoint with significant implications for future HCC immunotherapy.

The cell adhesion molecule BOC, a member of the Ig superfamily, exerts a significant positive regulatory effect on myogenic differentiation.[25] Furthermore, BOC functions as a receptor for the sonic Hedgehog (HH) signal, playing a pivotal role in regulating axon guidance.[26] The interaction between all mammalian HH proteins and cell

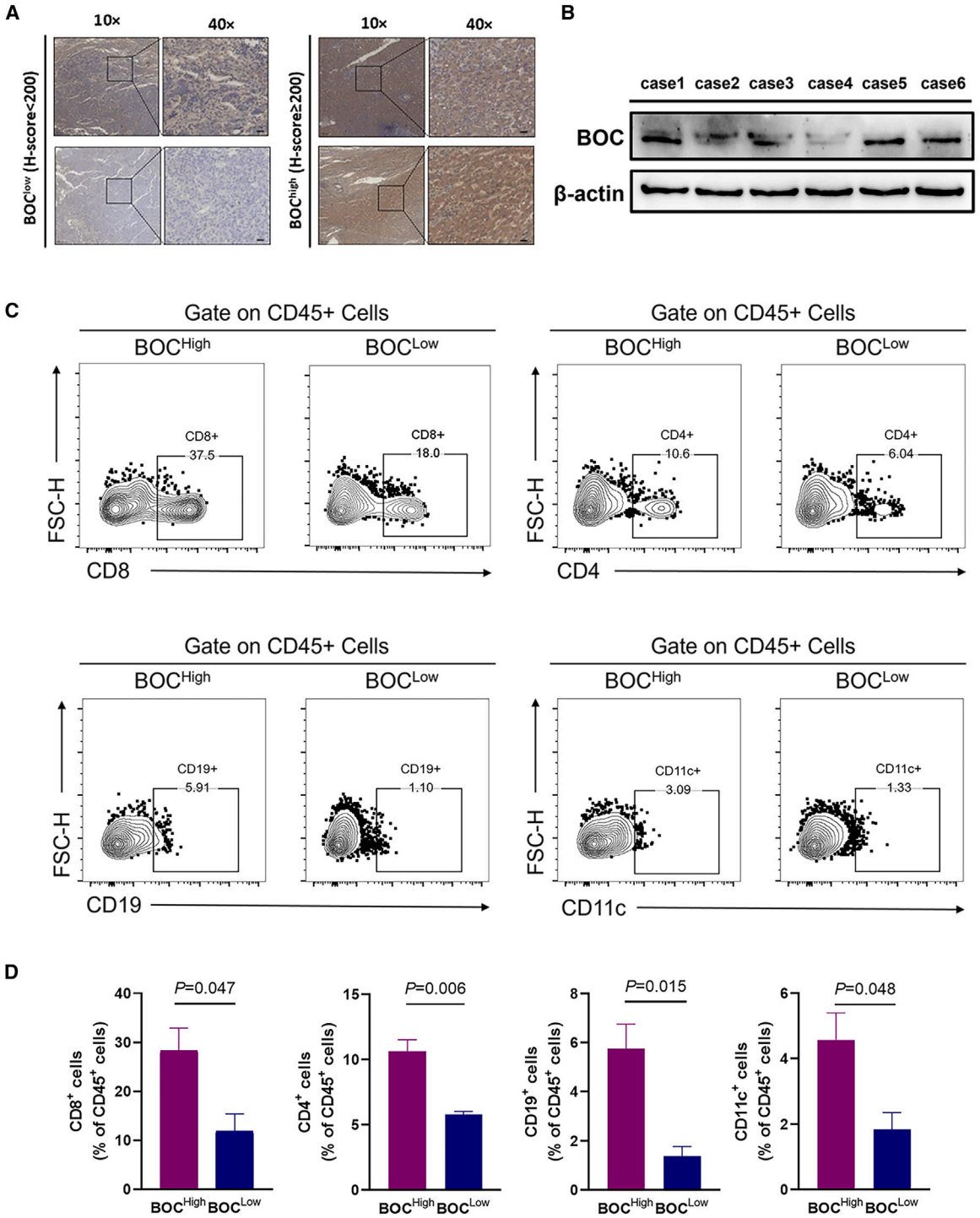

Figure 7. Elevated BOC expression correlates with favorable anti-PD-1 therapy outcomes and enhanced CD8⁺ T cell infiltration in HCC

(A) Representative images of the BOC protein's IHC staining density within the tissue specimens from 10 individuals with HCC, where each patient's staining outcome is evaluated by H-score, factoring in the cell percentage at distinct staining strengths. Scale bars, 25 μm. (B) Western blot showed the expression levels of BOC in tissues of six patients. (C and D) Flow cytometry analysis revealed the infiltration levels of $CD8^+$ T cells, $CD4^+$ T cells, B cells, and DCs in the tissues of the six patients. Results are expressed as mean ± SEM. *p* values were obtained through a two-sided unpaired Student's t test.

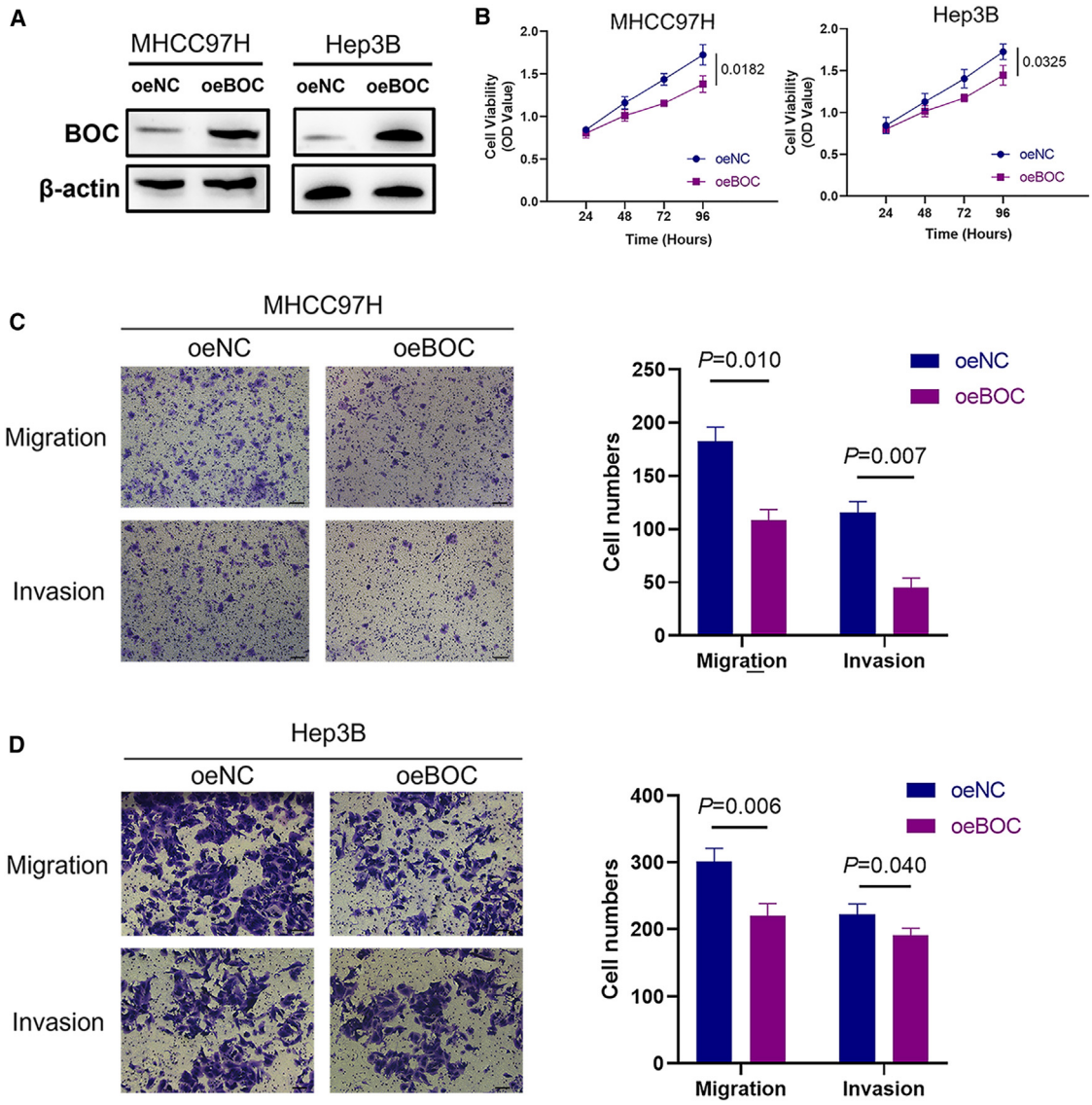

Figure 8. BOC overexpression attenuates proliferative and migratory capacities in HCC cell lines

(A) Western blot demonstrated the expression levels of BOC in MHCC97H (oeNC), Hep3B (oeNC), MHCC97H (oeBOC), and Hep3B (oeBOC) cells. oeBOC, overexpressed BOC; oeNC, overexpressed negative control. (B) CCK8 assay results showing cell viability for MHCC97H, Hep3B, MHCC97H (oeBOC), and Hep3B (oeBOC). (C and D) Transwell assays reveal the migration and invasion capabilities of MHCC97H and Hep3B cell lines between NC and BOC overexpression groups. Scale bars, 50 μm. Results are expressed as mean ± SEM. *p* values were obtained through a two-sided unpaired Student's t test.

adhesion molecules, including CDO and BOC, is highly conserved.[27] The HH signaling pathway is implicated in the accelerated progression of malignancies and poor prognosis.[28] Notably, BOC overexpression has been linked to the metastatic invasion of breast cancer cells into the cerebral domain.[29] In pancreatic cancer, the targeted deletion of BOC in fibroblasts, in which it acts as a receptor for the HH signaling pathway, can significantly diminish the pathway's primary signal responsiveness. This attenuation has the potential to prevent the progression of malignancy, suggesting offering a promising avenue for therapeutic intervention.[30]

Despite the promising insights of our study, we acknowledge certain inherent limitations that warrant further discussion. The retrospective nature of our analysis, which relied on data extracted from public databases, presents several challenges. The datasets we used may not include the full spectrum of HCC responses to immunotherapy due to the limited scope and the potential for selection bias. This limitation highlights the need for future studies that incorporate larger, more diverse patient cohorts and prospective data collection to validate our findings. Additionally, our approach for identifying immune cell types within the TME was based on marker gene expression,

which, while frequently used, may not precisely reflect the actual cellular abundance or heterogeneity.[31] Advanced techniques, such as single-cell RNA sequencing, would provide more granular information on the immune landscape and could be used to confirm the accuracy of our classifications. Moreover, although our findings highlight the prognostic potential of BOC, VSTM1, and PRDM12, the functional roles of these genes in HCC and their interactions within the immune microenvironment remain to be fully elucidated. Further *in vivo* experiments and mechanistic studies are necessary to explore these pathways and validate their relevance in clinical settings. Finally, the predictive value of our proposed immune-related classification for HCC, particularly for guiding immunotherapy strategies, requires rigorous testing in clinical trials. Until such validation is performed, the clinical applicability of our findings should be interpreted with caution.

Nonetheless, this study has significant potential to impact the field of HCC immunotherapy by offering a novel immune-related classification that could be pivotal in tailoring more effective treatment strategies. The identification of BOC and VSTM1 as key prognostic genes not only increases our understanding of the molecular mechanisms underlying HCC but also provides new directions for the development of targeted therapies. By linking these biomarkers with the immune microenvironment, our research paves the way for the development of more personalized and precise treatment modalities. However, this study also highlights critical knowledge gaps that need to be addressed. The retrospective nature of our analysis, which relied heavily on publicly available datasets, highlights the need for more comprehensive and diverse HCC immunotherapy datasets. Additionally, further investigations are needed to understand how BOC influences the effectiveness of immunotherapy in HCC patients. In the future, well-designed *in vitro* and *in vivo* experiments should be conducted to explore and validate its role, with the ultimate goal of translating these findings into clinical practice. Other research should apply single-cell sequencing technologies to validate our findings *in vivo* and refine our proposed classification system. We anticipate a rapidly evolving landscape in the study of HCC and its immune microenvironment. Over the next 5 years, advances in immunogenomics and high-throughput sequencing technologies are likely to uncover new biomarkers and therapeutic targets. The integration of multi-omics approaches could lead to the development of more robust and nuanced immune classifications, enhancing the precision of immunotherapy treatments. Additionally, as the role of the TME in mediating treatment responses becomes clearer, we anticipate the emergence of novel combination therapies that synergize immunotherapy with other modalities.

In summary, our research delineated two distinct immune subtypes of HCC, each characterized by a unique immunogenomic profile. We elucidated the potential of BOC as a novel biomarker of the prognosis and response to immunotherapy of HCC. However, the findings are preliminary and need to be validated in clinical trials; additionally, further investigation into the underlying molecular mechanisms is warranted.

MATERIALS AND METHODS

Data collection and operation

For this study, mRNA expression data in FPKM format, along with clinical information, were obtained from TCGA database, comprising 371 HCC cases and 50 normal samples. Additionally, extensive survival data for 72 HCC cases were acquired from the ICGC database. The analysis was further enriched by incorporating 115 HCC samples from the GSE76427 dataset available on the GEO platform.

Identification of HCC immunity subtypes

Extending prior investigations, 29 immunogenomic profiles were meticulously chosen to ascertain the immune status in individual patients.[32] Abundance levels in each HCC sample were quantified through ssGSEA, utilizing the Gene Set Variation Analysis (GSVA) package.[33,34] Hierarchical clustering analysis, conducted with the consensusclusterplus R package, enabled the stratification of patients into subgroups of high and low immunity, based on their ssGSEA scores corresponding to these immune profiles.[35,36]

Assessment of ESTIMATE score, TIS, and immune cell infiltration

The ESTIMATE algorithm was performed to quantify the immune and stromal cell populations within the TME, which yielded immune scores, stromal scores, and composite ESTIMATE scores.[37] These scores reflected the degree of immune and stromal cell infiltration as well as tumor purity. Additionally, the TIS, a genomic marker predictive of immunotherapy response,[38] was applied to assess potential immunotherapeutic responses in our cohort. The fractions of tumor-infiltrating immune cells were evaluated via the CIBERSORT and TIMER 2.0 algorithms.[39,40] The KEGG pathways and Hallmark gene sets were sourced from the Molecular Signatures Database (MSigDB). The GSEA was conducted using the GSVA package.[34,41,42]

Kaplan-Meier survival analysis between immunity subtypes and identification of core prognostic genes

Prognostic differences in DFS, PFS, and OS between the two immune subtypes were assessed using Kaplan-Meier survival curves, generated with the survival package in R. DEGs were identified by comparing tumor tissues with normal counterparts and between immune subtypes. The criteria for DEG selection were set at $|\log2\ FC| > 1$ and FDR <0.05. Subsequently, genes with significant prognostic potential were identified through a two-step process: first, a univariate Cox regression analysis was performed, followed by a LASSO-based Cox regression analysis using the glmnet package in R. This approach allowed for the identification of key genes associated with patient outcomes while minimizing overfitting.[43] The intersection of genes significantly correlated with DFS, PFS, and OS facilitated the delineation of core prognostic genes.

Correlation analysis between three hub gene expression and immune cell infiltration and the validation of immunotherapy response

Spearman's correlation analysis was employed to analyze the linkage between the expression levels of three hub genes and the fraction of

immune cells, as well as their expression with immune checkpoint genes. The immunotherapy response prediction of three hub genes was validated in an advanced or metastatic urothelial carcinoma cohort undergoing anti-PD-L1 therapy (Liu et al. cohort).[44] IHC staining and scoring were performed to determine the correlation between BOC expression levels and the efficacy of ICIs in patients with HCC. HCC tissue specimens were procured from individuals undergoing curative resection at Xijing Hospital. None of the patients received preoperative anticancer therapies. The ethics committee of Xijing Hospital granted ethical clearance (ethics no.: KY20232147-C-1) for the research. All participants provided informed consent, as per the requisite ethical guidelines. The IHC protocol was meticulously followed using formalin-fixed, paraffin-embedded HCC samples. BOC antibodies (ABclonal, China) were used, and the presence of antigen was visualized with 3,3′-diaminobenzidine (brand name DAB+) chromogen. In the quantitative analysis, the focus was on determining the proportion of positively stained cells and evaluating the staining intensity observed in representative fields. To quantify BOC expression in HCC tissues, the H-score methodology was employed. The intensity of staining was categorized as follows: 0 (no staining), 1+ (weak staining), 2+ (moderate staining), and 3+ (strong staining).[45] A visual appraisal was conducted to determine the percentage of cells within each staining intensity level. The H-score was computed using the formula H = 100 × (% of 1+ cells) + 200 × (% of 2+ cells) + 300 × (% of 3+ cells). Scores ranged from 0 to 300, with an H-score <200 indicating low BOC expression and a score of $\geq$200 signifying high BOC expression.

Cell studies

The evaluation of cell migration and invasion was conducted using transwell chambers featuring an 8-μm pore size (Corning, USA) and matrix gel (R&D Systems, USA). In the upper chamber, 50,000 cells were introduced in 200 μL serum-free medium. The lower chamber received 600 μL complete culture medium containing 10% fetal bovine serum. Following 24 h of incubation at 37°C, migrated cells on the bottom surface of the membrane were subjected to fixation and staining with crystal violet, and their quantification was carried out with the aid of an Olympus microscope.

Western blots

Cells were lysed using radioimmunoprecipitation assay buffer (Biosharp, China) supplemented with protease inhibitors (NCM, China). Protein concentrations were determined using the bicinchoninic acid (BCA) assay (Pierce BCA, Thermo Scientific, USA) according to the manufacturer's instructions. Equal amounts of protein were separated by SDS-PAGE and transferred onto polyvinylidene difluoride membranes. Non-specific binding was blocked by incubating the membranes with 5% non-fat milk in Tris-buffered saline containing 0.1% Tween 20 for 90 min at room temperature. The membranes were then probed with primary antibodies overnight at 4°C, followed by incubation with horseradish peroxidase-conjugated secondary antibodies for 1 h at room temperature. Protein bands were visualized using an enhanced chemiluminescence detection system and imaged.

Flow cytometry

Upon acquisition of human HCC tissue samples, dissociation into single-cell suspensions was achieved using the Human Tumor Tissue Dissociation Kit (Miltenyi Biotec, Germany) in accordance with the manufacturer's protocol, employing the GentleMACS Octo Dissociator with Heaters (Miltenyi Biotec). Following dissociation, protein extraction and flow cytometry analysis were performed on single-cell suspensions derived from the tissues of six patients to quantify the proportions of $CD4^+$ T cells, $CD8^+$ T cells, DCs, and B cells after fluorescent antibody (BioLegend, USA) labeling. These populations were subsequently identified and quantified via flow cytometry using a Beckman Coulter system (USA).

Statistical analyses

Comparative analysis of clinical characteristics across immune subtypes was facilitated by the chi-squared test. The Spearman correlation test was utilized to assess associations among numerical variables. For the comparison of variable groups, the selection between the parametric Student's t test and the nonparametric Wilcoxon test was based on the data distribution. All bioinformatic analyses were executed using R software (version 4.0.5), considering a two-sided p-value below 0.05 as indicative of statistical significance in all tests.

DATA AND CODE AVAILABILITY

All other data are available in the main text or in the supplemental information.

ACKNOWLEDGMENTS

The research received financial support from the Xijing Hospital Clinical Research Special Project - Key Projects (XJZT24LZ15), the scientific and technological innovation team of the Shaanxi Innovation Capability Support Plan (2023-CX-TD-67), and the Shaanxi Province Natural Science Basic Research Program (2021JQ-348). Acknowledgment is extended to the members of the TCGA, GEO, and ICGC databases for their provision of a platform that facilitates data acquisition and information sharing.

AUTHOR CONTRIBUTIONS

H.-M.Z. contributed to the research design, manuscript review & editing, funding acquisition, and supervision. Y.-P.L., L.-H.W., and X.-X.W. were responsible for data analysis, conducting the cell experiments, performing IHC, and writing the original draft. H.J., Y.Y., and Q.Z. curated the data and prepared the figures and tables.

DECLARATION OF INTERESTS

The authors declare no competing interests.

SUPPLEMENTAL INFORMATION

Supplemental information can be found online at https://doi.org/10.1016/j.omton.2024.200890.

REFERENCES

1. Bray, F., Laversanne, M., Sung, H., Ferlay, J., Siegel, R.L., Soerjomataram, I., and Jemal, A. (2024). Global cancer statistics 2022: GLOBOCAN estimates of incidence and mortality worldwide for 36 cancers in 185 countries. CA. Cancer J. Clin. *74*, 229–263. https://doi.org/10.3322/caac.21834.

2. Chan, S.L., Ryoo, B.Y., Mo, F., Chan, L.L., Cheon, J., Li, L., Wong, K.H., Yim, N., Kim, H., and Yoo, C. (2024). Multicentre phase II trial of cabozantinib in patients with hepatocellular carcinoma after immune checkpoint inhibitor treatment. J. Hepatol. *81*, 258–264. https://doi.org/10.1016/j.jhep.2024.03.033.

3. Rizzo, A., Ricci, A.D., and Brandi, G. (2022). Trans-Arterial Chemoembolization Plus Systemic Treatments for Hepatocellular Carcinoma: An Update. J. Pers. Med. *12*, 1788. https://doi.org/10.3390/jpm12111788.

4. Rizzo, A., Dadduzio, V., Ricci, A.D., Massari, F., Di Federico, A., Gadaleta-Caldarola, G., and Brandi, G. (2022). Lenvatinib plus pembrolizumab: the next frontier for the treatment of hepatocellular carcinoma? Expert Opin. Investig. Drugs *31*, 371–378. https://doi.org/10.1080/13543784.2021.1948532.

5. Sangro, B., Chan, S.L., Kelley, R.K., Lau, G., Kudo, M., Sukeepaisarnjaroen, W., Yarchoan, M., De Toni, E.N., Furuse, J., Kang, Y.K., et al. (2024). Four-year overall survival update from the phase III HIMALAYA study of tremelimumab plus durvalumab in unresectable hepatocellular carcinoma. Ann. Oncol. *35*, 448–457. https://doi.org/10.1016/j.annonc.2024.02.005.

6. Rizzo, A., Mollica, V., Tateo, V., Tassinari, E., Marchetti, A., Rosellini, M., De Luca, R., Santoni, M., and Massari, F. (2023). Hypertransaminasemia in cancer patients receiving immunotherapy and immune-based combinations: the MOUSEION-05 study. Cancer Immunol. Immunother. *72*, 1381–1394. https://doi.org/10.1007/s00262-023-03366-x.

7. Yang, X., Yang, C., Zhang, S., Geng, H., Zhu, A.X., Bernards, R., Qin, W., Fan, J., Wang, C., and Gao, Q. (2024). Precision treatment in advanced hepatocellular carcinoma. Cancer Cell *42*, 180–197. https://doi.org/10.1016/j.ccell.2024.01.007.

8. Tabrizian, P., Abdelrahim, M., and Schwartz, M. (2024). Immunotherapy and transplantation for hepatocellular carcinoma. J. Hepatol. *80*, 822–825. https://doi.org/10.1016/j.jhep.2024.01.011.

9. Greten, T.F., Villanueva, A., Korangy, F., Ruf, B., Yarchoan, M., Ma, L., Ruppin, E., and Wang, X.W. (2023). Biomarkers for immunotherapy of hepatocellular carcinoma. Nat. Rev. Clin. Oncol. *20*, 780–798. https://doi.org/10.1038/s41571-023-00816-4.

10. Guven, D.C., Sahin, T.K., Erul, E., Rizzo, A., Ricci, A.D., Aksoy, S., and Yalcin, S. (2022). The association between albumin levels and survival in patients treated with immune checkpoint inhibitors: A systematic review and meta-analysis. Front. Mol. Biosci. *9*, 1039121. https://doi.org/10.3389/fmolb.2022.1039121.

11. Sahin, T.K., Rizzo, A., Aksoy, S., and Guven, D.C. (2024). Prognostic Significance of the Royal Marsden Hospital (RMH) Score in Patients with Cancer: A Systematic Review and Meta-Analysis. Cancers *16*, 1835. https://doi.org/10.3390/cancers16101835.

12. Yu, S.J. (2023). Immunotherapy for hepatocellular carcinoma: Recent advances and future targets. Pharmacol. Ther. *244*, 108387. https://doi.org/10.1016/j.pharmthera.2023.108387.

13. Donne, R., and Lujambio, A. (2023). The liver cancer immune microenvironment: Therapeutic implications for hepatocellular carcinoma. Hepatology *77*, 1773–1796. https://doi.org/10.1002/hep.32740.

14. Oura, K., Morishita, A., Tani, J., and Masaki, T. (2021). Tumor Immune Microenvironment and Immunosuppressive Therapy in Hepatocellular Carcinoma: A Review. Int. J. Mol. Sci. *22*, 5801. https://doi.org/10.3390/ijms22115801.

15. Zhang, X., Wei, Z., Yong, T., Li, S., Bie, N., Li, J., Li, X., Liu, H., Xu, H., Yan, Y., et al. (2023). Cell microparticles loaded with tumor antigen and resiquimod reprogram tumor-associated macrophages and promote stem-like CD8(+) T cells to boost anti-PD-1 therapy. Nat. Commun. *14*, 5653. https://doi.org/10.1038/s41467-023-41438-9.

16. Riera-Domingo, C., Audigé, A., Granja, S., Cheng, W.-C., Ho, P.-C., Baltazar, F., Stockmann, C., and Mazzone, M. (2020). Immunity, Hypoxia, and Metabolism–the Ménage à Trois of Cancer: Implications for Immunotherapy. Physiol. Rev. *100*, 1–102. https://doi.org/10.1152/physrev.00018.2019.

17. Passaro, A., Al Bakir, M., Hamilton, E.G., Diehn, M., André, F., Roy-Chowdhuri, S., Mountzios, G., Wistuba, I.I., Swanton, C., and Peters, S. (2024). Cancer biomarkers: Emerging trends and clinical implications for personalized treatment. Cell *187*, 1617–1635. https://doi.org/10.1016/j.cell.2024.02.041.

18. Kumagai, S., Itahashi, K., and Nishikawa, H. (2024). Regulatory T cell-mediated immunosuppression orchestrated by cancer: towards an immuno-genomic paradigm for precision medicine. Nat. Rev. Clin. Oncol. *21*, 337–353. https://doi.org/10.1038/s41571-024-00870-6.

19. Guan, X., Xu, Z.Y., Chen, R., Qin, J.J., and Cheng, X.D. (2020). Identification of an Immune Gene-Associated Prognostic Signature and Its Association With a Poor Prognosis in Gastric Cancer Patients. Front. Oncol. *10*, 629909. https://doi.org/10.3389/fonc.2020.629909.

20. Jiang, Y.Z., Ma, D., Suo, C., Shi, J., Xue, M., Hu, X., Xiao, Y., Yu, K.D., Liu, Y.R., Yu, Y., et al. (2019). Genomic and Transcriptomic Landscape of Triple-Negative Breast Cancers: Subtypes and Treatment Strategies. Cancer Cell *35*, 428–440.e5. https://doi.org/10.1016/j.ccell.2019.02.001.

21. Abou-Alfa, G.K., Lau, G., Kudo, M., Chan, S.L., Kelley, R.K., Furuse, J., Sukeepaisarnjaroen, W., Kang, Y.K., Van Dao, T., De Toni, E.N., et al. (2022). Tremelimumab plus Durvalumab in Unresectable Hepatocellular Carcinoma. NEJM Evid. *1*, EVIDoa2100070. https://doi.org/10.1056/EVIDoa2100070.

22. Ali, H.R., Provenzano, E., Dawson, S.J., Blows, F.M., Liu, B., Shah, M., Earl, H.M., Poole, C.J., Hiller, L., Dunn, J.A., et al. (2014). Association between CD8+ T-cell infiltration and breast cancer survival in 12,439 patients. Ann. Oncol. *25*, 1536–1543. https://doi.org/10.1093/annonc/mdu191.

23. Garnelo, M., Tan, A., Her, Z., Yeong, J., Lim, C.J., Chen, J., Lim, K.H., Weber, A., Chow, P., Chung, A., et al. (2017). Interaction between tumour-infiltrating B cells and T cells controls the progression of hepatocellular carcinoma. Gut *66*, 342–351. https://doi.org/10.1136/gutjnl-2015-310814.

24. Xie, M., Li, T., Li, N., Li, J., Yao, Q., Han, W., and Ruan, G. (2015). VSTM-v1, a potential myeloid differentiation antigen that is downregulated in bone marrow cells from myeloid leukemia patients. J. Hematol. Oncol. *8*, 25. https://doi.org/10.1186/s13045-015-0118-4.

25. Kang, J.S., Mulieri, P.J., Hu, Y., Taliana, L., and Krauss, R.S. (2002). BOC, an Ig superfamily member, associates with CDO to positively regulate myogenic differentiation. EMBO J. *21*, 114–124. https://doi.org/10.1093/emboj/21.1.114.

26. Okada, A., Charron, F., Morin, S., Shin, D.S., Wong, K., Fabre, P.J., Tessier-Lavigne, M., and McConnell, S.K. (2006). Boc is a receptor for sonic hedgehog in the guidance of commissural axons. Nature *444*, 369–373. https://doi.org/10.1038/nature05246.

27. Kavran, J.M., Ward, M.D., Oladosu, O.O., Mulepati, S., and Leahy, D.J. (2010). All mammalian Hedgehog proteins interact with cell adhesion molecule, down-regulated by oncogenes (CDO) and brother of CDO (BOC) in a conserved manner. J. Biol. Chem. *285*, 24584–24590. https://doi.org/10.1074/jbc.M110.131680.

28. Jing, J., Wu, Z., Wang, J., Luo, G., Lin, H., Fan, Y., and Zhou, C. (2023). Hedgehog signaling in tissue homeostasis, cancers, and targeted therapies. Signal Transduct. Targeted Ther. *8*, 315. https://doi.org/10.1038/s41392-023-01559-5.

29. Pedrosa, R.M.S.M., Wismans, L.V., Sinke, R., van der Weiden, M., van Eijck, C.H.J., Kros, J.M., and Mustafa, D.A.M. (2021). Differential Expression of BOC, SPOCK2, and GJD3 Is Associated with Brain Metastasis of ER-Negative Breast Cancers. Cancers *13*, 2982. https://doi.org/10.3390/cancers13122982.

30. Mathew, E., Zhang, Y., Holtz, A.M., Kane, K.T., Song, J.Y., Allen, B.L., and Pasca di Magliano, M. (2014). Dosage-dependent regulation of pancreatic cancer growth and angiogenesis by hedgehog signaling. Cell Rep. *9*, 484–494. https://doi.org/10.1016/j.celrep.2014.09.010.

31. Kwak, M., Erdag, G., and Slingluff, C.L., Jr. (2020). Gene expression analysis in formalin fixed paraffin embedded melanomas is associated with density of corresponding immune cells in those tissues. Sci. Rep. *10*, 18336. https://doi.org/10.1038/s41598-020-74996-9.

32. He, Y., Jiang, Z., Chen, C., and Wang, X. (2018). Classification of triple-negative breast cancers based on Immunogenomic profiling. J. Exp. Clin. Cancer Res. *37*, 327. https://doi.org/10.1186/s13046-018-1002-1.

33. Subramanian, A., Tamayo, P., Mootha, V.K., Mukherjee, S., Ebert, B.L., Gillette, M.A., Paulovich, A., Pomeroy, S.L., Golub, T.R., Lander, E.S., and Mesirov, J.P. (2005). Gene set enrichment analysis: a knowledge-based approach for interpreting genome-wide expression profiles. Proc. Natl. Acad. Sci. USA *102*, 15545–15550. https://doi.org/10.1073/pnas.0506580102.

34. Hanzelmann, S., Castelo, R., and Guinney, J. (2013). GSVA: gene set variation analysis for microarray and RNA-seq data. BMC Bioinf. *14*, 7. https://doi.org/10.1186/1471-2105-14-7.

35. Seiler, M., Huang, C.C., Szalma, S., and Bhanot, G. (2010). ConsensusCluster: a software tool for unsupervised cluster discovery in numerical data. OMICS *14*, 109–113. https://doi.org/10.1089/omi.2009.0083.

36. Wilkerson, M.D., and Hayes, D.N. (2010). ConsensusClusterPlus: a class discovery tool with confidence assessments and item tracking. Bioinformatics *26*, 1572–1573. https://doi.org/10.1093/bioinformatics/btq170.

37. Yoshihara, K., Shahmoradgoli, M., Martínez, E., Vegesna, R., Kim, H., Torres-Garcia, W., Treviño, V., Shen, H., Laird, P.W., Levine, D.A., et al. (2013). Inferring tumour purity and stromal and immune cell admixture from expression data. Nat. Commun. *4*, 2612. https://doi.org/10.1038/ncomms3612.

38. Ayers, M., Lunceford, J., Nebozhyn, M., Murphy, E., Loboda, A., Kaufman, D.R., Albright, A., Cheng, J.D., Kang, S.P., Shankaran, V., et al. (2017). IFN-gamma-related mRNA profile predicts clinical response to PD-1 blockade. J. Clin. Invest. *127*, 2930–2940. https://doi.org/10.1172/JCI91190.

39. Li, T., Fu, J., Zeng, Z., Cohen, D., Li, J., Chen, Q., Li, B., and Liu, X.S. (2020). TIMER2.0 for analysis of tumor-infiltrating immune cells. Nucleic Acids Res. *48*, W509–W514. https://doi.org/10.1093/nar/gkaa407.

40. Newman, A.M., Liu, C.L., Green, M.R., Gentles, A.J., Feng, W., Xu, Y., Hoang, C.D., Diehn, M., and Alizadeh, A.A. (2015). Robust enumeration of cell subsets from tissue expression profiles. Nat. Methods *12*, 453–457. https://doi.org/10.1038/nmeth.3337.

41. Kanehisa, M., Furumichi, M., Tanabe, M., Sato, Y., and Morishima, K. (2017). KEGG: new perspectives on genomes, pathways, diseases and drugs. Nucleic Acids Res. *45*, D353–D361. https://doi.org/10.1093/nar/gkw1092.

42. Liberzon, A., Birger, C., Thorvaldsdóttir, H., Ghandi, M., Mesirov, J.P., and Tamayo, P. (2015). The Molecular Signatures Database (MSigDB) hallmark gene set collection. Cell Syst. *1*, 417–425. https://doi.org/10.1016/j.cels.2015.12.004.

43. Blanco, J.L., Porto-Pazos, A.B., Pazos, A., and Fernandez-Lozano, C. (2018). Prediction of high anti-angiogenic activity peptides in silico using a generalized linear model and feature selection. Sci. Rep. *8*, 15688. https://doi.org/10.1038/s41598-018-33911-z.

44. Liu, D., Schilling, B., Liu, D., Sucker, A., Livingstone, E., Jerby-Arnon, L., Zimmer, L., Gutzmer, R., Satzger, I., Loquai, C., et al. (2019). Integrative molecular and clinical modeling of clinical outcomes to PD1 blockade in patients with metastatic melanoma. Nat. Med. *25*, 1916–1927. https://doi.org/10.1038/s41591-019-0654-5.

45. Jin, H., Shi, Y., Lv, Y., Yuan, S., Ramirez, C.F.A., Lieftink, C., Wang, L., Wang, S., Wang, C., Dias, M.H., et al. (2021). EGFR activation limits the response of liver cancer to lenvatinib. Nature *595*, 730–734. https://doi.org/10.1038/s41586-021-03741-7.